Progress In Electromagnetics Research M, Vol. 51, 165–173, 2016

Application of Group Theory for Computation Reduction in Microwave Imaging of Human Breast Model at 500 MHz

Hardik N. Patel* and Deepak K. Ghodgaonkar

Abstract—In microwave imaging, accuracy of breast cancer detection depends on complex permittivity profile reconstruction in breast. Inverse scattering problem is solved to reconstruct complex permittivity profile of breast. In this paper, computation time to solve inverse scattering problem is reduced by exploiting symmetry present in breast models using group theory. Forward problem is solved using method of moments. Levenberg-Marquardt algorithm is used to solve inverse scattering problem with and without group theory. Results show that computation time is reduced considerably by exploiting symmetry present in breast models using group theory. At higher SNR, error in complex permittivity reconstruction with group theory is approximately same as error without group theory.

1. INTRODUCTION

Breast cancer detection research using microwave imaging is growing rapidly due to non-ionizing nature of microwave radiation. However, there are several pending research challenges in this research area. Microwave signal is transmitted by antenna arrays surrounding human breast. This signal then interacts with the breast tissues. According to dielectric profile of breast tissues, signal is scattered and received at receivers surrounding human breast. Now, based on this received signal dielectric profile of breast tissues is reconstructed in inverse problem. Two breast models are used in this paper. First model is used for explanation of group theory concepts. Second model is used in simulation. Forward problem is solved by using moment-method formulation of electric field integral equation [1–5]. Group theory is applied on matrices to exploit symmetry. Now, Inverse scattering problem is formulated in the presence of noise. This formulated problem is solved by using Levenberg-Marquardt algorithm. An overview of previous work is given below which form base for this research paper. Computation reduction using group theory in human breast model is reported in [1]. Phase unwrapping and log-phase formulation is used to implement 3-D microwave imaging of breast cancer in [2]. Method of moments based electric field calculation inside biological body is shown in detail [3]. Matrix formulation of electromagnetic problem is given using method of moments in [4]. Microwave imaging of human chest 36-cell model is given with all technical details in [5]. Computation cost of matrix inversion in electromagnetic imaging is reduced by exploiting symmetry using group theory in [6, 7]. Pseudo inverse transformation is applied on matrix to solve electromagnetic problem in [8]. Dielectric profile reconstruction of human arm and horse kidney is shown using models in [9]. Dielectric profile reconstruction using stochastic technique known as simulated annealing is described greatly in [10]. Multi frequency scattering data is used for shape and location reconstruction in [11]. A classical model driven approach is given for biomedical applications in [12]. Different stochastic methods, to solve inverse scattering problem for microwave imaging are reviewed in [13]. Singular value decomposition is used to solve inverse scattering problem in [14]. Hybrid reconstruction technique using Levenberg-Marquardt and genetic algorithm is described in detail [15]. Gauss-Newton and conjugate gradient least square algorithms are used to solve

Received 5 August 2016, Accepted 20 October 2016, Scheduled 4 November 2016
* Corresponding author: Hardik N. Patel (hardikec2003@gmail.com).
The authors are with the RF & Wireless Group, DA-IICT, Gandhinagar, Gujarat, India.

inverse scattering problem for breast cancer imaging in [16]. The next sections are problem formulation, human breast models, group theory and symmetry, simulation parameters and noise, Inverse scattering problem formulation, results and conclusion. The effects of number of cells, total volume, and symmetry on complex permittivity reconstruction are investigated in this paper.

2. PROBLEM FORMULATION

Microwave signal transmitted by antennas is scattered by breast tissues according to their dielectric profiles. Scattered field at receiver locations is calculated as given in [3, 18].

$$\vec{E}^s(\vec{r}) = \iiint G(\vec{r},\vec{r}') \cdot \vec{J}(\vec{r}')dv' \tag{1}$$

In order to obtain Eq. (2), values of Green's function $G(\vec{r},\vec{r}')$ and polarization current density $\vec{J}(\vec{r}')$ are substituted into Eq. (1).

$$\vec{E}^s(\vec{r}) = k_\varepsilon^2 \iiint (\varepsilon_r(\vec{r}') - 1)\vec{E}(\vec{r}') \left[I + \frac{\nabla\nabla}{k_\varepsilon^2}\right] \frac{e^{-jk_\varepsilon R}}{4\pi R} dv' \tag{2}$$

In (2), $\vec{E}(\vec{r}')$ is internal electric field at cell location $\vec{r}'$, $\nabla\nabla$ the dyadic, R the distance between cell centroid and receiver location, and K_ε a wave-number of surrounding medium. Electric field relationship is given using Eq. (3).

$$\vec{E}(\vec{r}) = \vec{E}^{inc}(\vec{r}) + \vec{E}^s(\vec{r}) \tag{3}$$

In Eq. (3), $\vec{E}$ is the total electric field, $\vec{E}^{inc}$ the incident electric field, and $\vec{E}^s$ the scattered electric field. Now, Eq. (4) is obtained using Eqs. (2) and (3) [5, 7].

$$-\vec{E}^i(\vec{r}) = k_\varepsilon^2 \iiint (\varepsilon_r(\vec{r}') - 1)\vec{E}(\vec{r}') \left[I + \frac{\nabla\nabla}{k_\varepsilon^2}\right] \frac{e^{-jk_\varepsilon R}}{4\pi R} dv' - \vec{E}(\vec{r}) \tag{4}$$

If the body is divided in N cubical cells, then internal electric field within dielectric body may be expanded as

$$\vec{E}(\vec{r}) = \sum_{l=1}^{N} \vec{E}_l \tag{5}$$

In Eq. (5), $\vec{E}_l$ represents three orthogonal components of internal electric field inside lth cell. Volume integral of Green's function is converted into matrix by using Eq. (6) [4, 7].

$$G_{ml}^{xx} = \frac{e^{-jk_\varepsilon R_{ml}}}{k_\varepsilon R_{ml}}[\sin(k_\varepsilon a) - k_\varepsilon a \cdot \cos(k_\varepsilon a)] + \sum_{i=1}^{2}(-1)^i \int_{Y_l-\frac{\Delta l}{2}}^{Y_l+\frac{\Delta l}{2}} \int_{Z_l-\frac{\Delta l}{2}}^{Z_l+\frac{\Delta l}{2}} \frac{(1+jk_\varepsilon R')}{4\pi R'^2} e^{-jk_\varepsilon R'}(x_m - x')dy'dz' \tag{6}$$

where $R' = [(x_m - x')^2 + (y_m - y')^2 + (z_m - z')^2]^{1/2}$, $\vec{r}' = \vec{r}_l + (-1)^i \frac{\Delta l}{2}\vec{U}_j$, where $\vec{U}_j$, $j = 1, 2, 3$ for unit vectors in $\hat{x}$, $\hat{y}$, and $\hat{z}$ directions, respectively. In Eq. (6), R_{ml} is distance between receiver locations m and cell locations l, $a = (3/4\pi)^{1/3}\Delta l$, where Δl is the length of each cell. Equation (7) is obtained by using Eqs. (2), (5), and (6).

$$\vec{E}^s = B_1 R^\varepsilon \vec{E} \tag{7}$$

B_1 is obtained by solving volume integral of Green's function. Size of B_1 is $3N \times 3N$. $\vec{E}^s$ is scattered electric field matrix of size $3N \times 1$. R^ε is diagonal matrix of size $3N \times 3N$ which contains complex permittivity values $\varepsilon_r - 1$ for various cells. $\vec{E}$ is internal electric field matrix of size $3N \times 1$. Equation (8) is obtained by using Eqs. (4), (5), and (6).

$$-\vec{E}^i = (A_1 R^\varepsilon - I)\vec{E} \tag{8}$$

$\vec{E}^i$ is incident electric field matrix of size $3N \times 1$, and A_1 is calculated by solving volume integral of Green's function. Incident field due to transmitter is calculated at each cell centroid when body is not present. Once $\vec{E}^i$ is known, internal field matrix $\vec{E}$ is calculated by using Eq. (8). Scattered field matrix is calculated using Eq. (7), which is known as forward problem. In Eq. (7), problem of determining unknown complex permittivity matrix R^ε from the knowledge of $\vec{E}^s$ and $\vec{E}^i$ is known as inverse scattering problem. In this paper, Iterative scheme is used to solve ill-posed inverse problem.

3. HUMAN BREAST MODELS

First model is given in Fig. 1 [1]. Symmetry exploitation is explained by using this model.

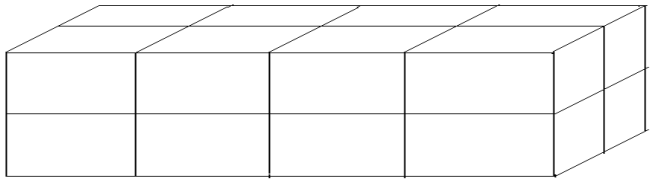

Figure 1. First breast model.

The above model is shown as the top and bottom layers in Fig. 2 and Fig. 3, respectively with cell numbers and transceiver numbers [1]. These transceiver works as transmitter and receiver. Incident field due to all transmitters is calculated at each cell centroid location.

Figure 4 shows a 64 cell breast model [1]. Volume of 512 cm^3 is assumed for this model. Nipple is represented by layer 1. Skin, fatty tissues, milk ducts and fibro glandular tissues are represented by layer 2. Skin, fatty tissues, fibro glandular tissues, and lobules are represented by layer 3. Layer 4 represents skin, fatty tissues, fibro glandular tissues, cancerous tissues, pectoralis muscles and chest wall. Layer 1 has 4 cells, layer 2 16 cells, layer 3 20 cells and layer 4 24 cells in three dimensions. Simulation is done using this 64 cell model. The number of cells is increased in simulation process, but the volume is fixed.

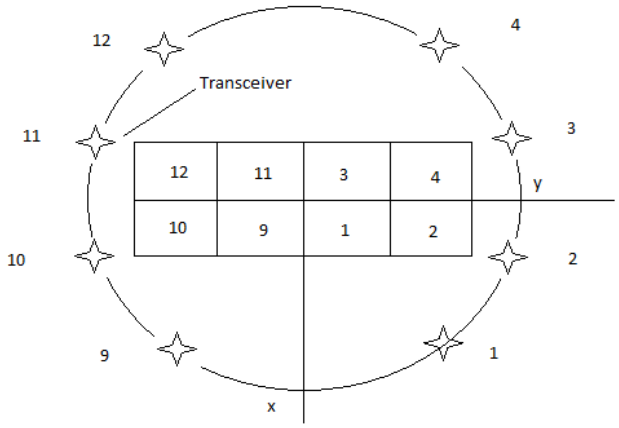

Figure 2. Top layer of 16 cell breast model.

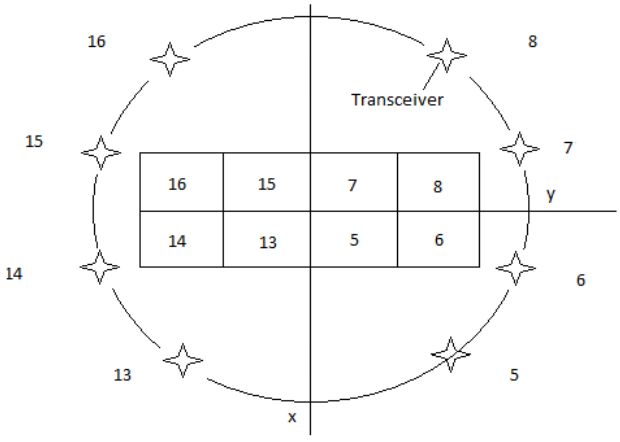

Figure 3. Bottom layer of 16 cell breast model.

Cell and receiver numbers pattern is same as the first model. Complex permittivity is calculated by using Eq. (9).

$$\varepsilon_r^*(\omega) = \varepsilon_r - j\frac{\sigma}{\omega\varepsilon_0} \tag{9}$$

In Equation (9), $\varepsilon_r^*(\omega)$ is the complex relative permittivity as function of angular frequency ω, σ the conductivity, ε_0 the permittivity of free space, and ε_r the relative permittivity [19]. Different breast

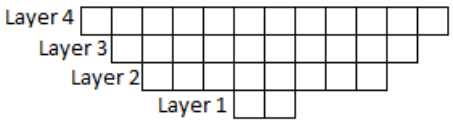

Figure 4. Human breast model in 2-D.

Table 1. Complex permittivity values of different breast tissues at 500 MHz.

Biological Tissues	Complex Permittivity
Breast Fat	$5.5 - j1.32$
Skin Dry	$44.92 - j26.19$
Skin Wet	$48.62 - j25.32$
Glandular tissues	$20 - j14.38$
Nipple	$45 - j25.16$
Blood vessels	$46.23 - j21.07$
Cancerous tissues	$65 - j32$

tissues' complex permittivity values at 500 MHz are given in Table 1 [17]. Volume averaged complex permittivity is assigned based on the values given in Table 1.

4. GROUP THEORY AND SYMMETRY

The structure of matrix B_1 is shown in Eq. (10). Matrix B_1 is volume integral of Green's function. Rows of B_1 represent receivers. Columns of B_1 represent cells. In Eq. (10), m is the number of receivers and n the number of cells [7].

$$B_1 = \begin{bmatrix} b_{11} & b_{12} & \dots & b_{1n} \\ b_{21} & b_{22} & \dots & b_{2n} \\ b_{31} & b_{32} & \dots & b_{3n} \\ . & . & \dots & . \\ . & . & \dots & . \\ b_{m1} & b_{m2} & \dots & b_{mn} \end{bmatrix} \tag{10}$$

The structure of each sub matrix is shown in Eq. (11). Each sub-matrix is symmetric [6]. Symmetry present in matrix B_1 is exploited by group theory.

$$b_{mn} = \begin{bmatrix} b_{mn}^{xx} & b_{mn}^{xy} & b_{mn}^{xz} \\ b_{mn}^{yx} & b_{mn}^{yy} & b_{mn}^{yz} \\ b_{mn}^{zx} & b_{mn}^{zy} & b_{mn}^{zz} \end{bmatrix} \tag{11}$$

Symmetry present in measurement domain is exploited by group theory. The concept is given in [6, 7]. Equations (12), (13), and (14) represent operators of group theory.

$$R_1(x, y, z) = (-x, y, z) \tag{12}$$
$$R_2(x, y, z) = (x, -y, z) \tag{13}$$
$$R_3(x, y, z) = (x, y, -z) \tag{14}$$

Group multiplication table and octants are given in [6, 7] with great details. The group is shown by using Eq. (15).

$$G = \{I, R_1, R_2, R_3, R_1R_2, R_2R_3, R_1R_3, R_1R_2R_3\} \tag{15}$$

Unitary transformation matrix is formed by exploiting symmetry in cells and receivers as given in Fig. 2 and Fig. 3. Equation (10) represents structure of volume integral of Green's function matrix. Particular

receiver is represented by row of matrix. Cell is represented by column of matrix. Cell numbers vary from 1 to n. Receiver numbers vary from 1 to m. For next few lines, consider Fig. 2. Cell numbers 1, 2 and receiver numbers 1, 2 are represented by positive coordinates (x, y, z), which represent identity element of the above group. Cell numbers 3, 4 and receiver numbers 3, 4 are represented by coordinates $(-x, y, z)$. Only x is negative, which represents group element R_1. Similarly, cell numbers 5, 6 and receiver numbers 5, 6 are represented by coordinates $(x, y, -z)$ which represent group element R_3. Cell numbers 7, 8 and receiver numbers 7, 8 are represented by coordinates $(-x, y, -z)$ which represent $-R_2$. Cells and receivers of Fig. 3 are also combined and represented by one of the group elements. By this way, unitary transformation matrix V is formed [7]. Each element of this matrix is also a diagonal matrix. Diagonal matrix represents particular group element. Now block diagonalization is applied on matrices B_1, E and E^s using Eqs. (16), (17), and (18), respectively. Transformation matrix V is given by Eq. (19).

$$\overleftrightarrow{B}_{1b} = \overleftrightarrow{V} \times \overleftrightarrow{B}_1 \times \overleftrightarrow{V}^T \tag{16}$$

$$\overleftrightarrow{J}_b = \overleftrightarrow{V} \times \overleftrightarrow{J} \tag{17}$$

$$\overleftrightarrow{E^s}_b = \overleftrightarrow{V} \times \overleftrightarrow{E^s} \tag{18}$$

$$V = \frac{1}{2\sqrt{2}} \begin{pmatrix} +\overleftrightarrow{I}_s & +\overleftrightarrow{I}_{s1} & +\overleftrightarrow{I}_{s3} & -\overleftrightarrow{I}_{s2} & +\overleftrightarrow{I}_{s2} & -\overleftrightarrow{I}_{s3} & -\overleftrightarrow{I}_{s1} & -\overleftrightarrow{I}_s \\ +\overleftrightarrow{I}_s & +\overleftrightarrow{I}_{s1} & -\overleftrightarrow{I}_{s3} & +\overleftrightarrow{I}_{s2} & +\overleftrightarrow{I}_{s2} & -\overleftrightarrow{I}_{s3} & +\overleftrightarrow{I}_{s1} & +\overleftrightarrow{I}_s \\ +\overleftrightarrow{I}_s & -\overleftrightarrow{I}_{s1} & +\overleftrightarrow{I}_{s3} & +\overleftrightarrow{I}_{s2} & +\overleftrightarrow{I}_{s2} & +\overleftrightarrow{I}_{s3} & -\overleftrightarrow{I}_{s1} & +\overleftrightarrow{I}_s \\ +\overleftrightarrow{I}_s & -\overleftrightarrow{I}_{s1} & -\overleftrightarrow{I}_{s3} & -\overleftrightarrow{I}_{s2} & +\overleftrightarrow{I}_{s2} & +\overleftrightarrow{I}_{s3} & +\overleftrightarrow{I}_{s1} & -\overleftrightarrow{I}_s \\ +\overleftrightarrow{I}_s & +\overleftrightarrow{I}_{s1} & +\overleftrightarrow{I}_{s3} & -\overleftrightarrow{I}_{s2} & -\overleftrightarrow{I}_{s2} & +\overleftrightarrow{I}_{s3} & +\overleftrightarrow{I}_{s1} & +\overleftrightarrow{I}_s \\ +\overleftrightarrow{I}_s & +\overleftrightarrow{I}_{s1} & -\overleftrightarrow{I}_{s3} & +\overleftrightarrow{I}_{s2} & -\overleftrightarrow{I}_{s2} & +\overleftrightarrow{I}_{s3} & -\overleftrightarrow{I}_{s1} & -\overleftrightarrow{I}_s \\ +\overleftrightarrow{I}_s & -\overleftrightarrow{I}_{s1} & +\overleftrightarrow{I}_{s3} & +\overleftrightarrow{I}_{s2} & -\overleftrightarrow{I}_{s2} & -\overleftrightarrow{I}_{s3} & +\overleftrightarrow{I}_{s1} & -\overleftrightarrow{I}_s \\ +\overleftrightarrow{I}_s & -\overleftrightarrow{I}_{s1} & -\overleftrightarrow{I}_{s3} & -\overleftrightarrow{I}_{s2} & -\overleftrightarrow{I}_{s2} & -\overleftrightarrow{I}_{s3} & -\overleftrightarrow{I}_{s1} & +\overleftrightarrow{I}_s \end{pmatrix} \tag{19}$$

In the matrix given by Eq. (19),

$$\overleftrightarrow{I}_s = \text{diag} \cdot (\overleftrightarrow{I}_0, \overleftrightarrow{I}_0, \ldots, \overleftrightarrow{I}_0)$$
$$\overleftrightarrow{I}_{s1} = \text{diag} \cdot (\overleftrightarrow{I}_1, \overleftrightarrow{I}_1, \ldots, \overleftrightarrow{I}_1)$$
$$\overleftrightarrow{I}_{s2} = \text{diag} \cdot (\overleftrightarrow{I}_2, \overleftrightarrow{I}_2, \ldots, \overleftrightarrow{I}_2)$$
$$\overleftrightarrow{I}_{s3} = \text{diag} \cdot (\overleftrightarrow{I}_3, \overleftrightarrow{I}_3, \ldots, \overleftrightarrow{I}_3)$$

Size of above four matrices is equal to $(3N/2^3) \times (3N/2^3)$, where N is the total number of cells. Matrices used to construct $\overleftrightarrow{I}_s$, $\overleftrightarrow{I}_{s1}$, $\overleftrightarrow{I}_{s2}$, and $\overleftrightarrow{I}_{s3}$ are given below.

$$I_0 = \begin{pmatrix} 1 & 0 & 0 \\ 0 & 1 & 0 \\ 0 & 0 & 1 \end{pmatrix} \quad , \quad I_1 = \begin{pmatrix} -1 & 0 & 0 \\ 0 & 1 & 0 \\ 0 & 0 & 1 \end{pmatrix}$$

$$I_2 = \begin{pmatrix} 1 & 0 & 0 \\ 0 & -1 & 0 \\ 0 & 0 & 1 \end{pmatrix} \quad , \quad I_3 = \begin{pmatrix} 1 & 0 & 0 \\ 0 & 1 & 0 \\ 0 & 0 & -1 \end{pmatrix}$$

Because of group theory, we have to consider 8 matrices of $3N/8 \times 3N/8$ instead of $3N \times 3N$ B_1 matrix. Computational time and storage requirements are reduced by applying symmetry. Same approach is applied to the second breast model of Fig. 4. Group formation for the second model is given in Table 2.

For 64-cell model, the number of cells and corresponding group element used to represent them are shown in Table 2. This model is symmetric in x and y planes but not in z plane, so dummy cells and receivers are assumed for preserving symmetry. Unitary transformation matrix formation and block diagonalization procedure is the same as used for the first breast model. The sizes of matrices are different for both the models.

Table 2. Group formation for 64 cell model.

Number of cells	Corresponding group element
11	I
11	R_1
5	R_3
5	$-R_2$
11	R_2
11	$-R_3$
5	$-R_1$
5	$-I$

5. SIMULATION PARAMETERS AND NOISE

Two percent saline is used as surrounding medium to provide better matching. Short dipoles are used as trans-receivers. In Table 1, complex permittivity values are used to calculate volume averaged complex permittivity. Volume averaged permittivity values are assigned to centroid of each cell. Additive white Gaussian noise is added in scattered field using Eq. (20). After adding noise, inverse problem is solved without group theory as well as with group theory.

$$\vec{E}^s = B\vec{E} + n \tag{20}$$

In the above equation, n is AWGN noise vector with different signal to noise ratios. SNR varies from 20 dB to 60 dB. As a part of result, RMS value of error in complex permittivity is calculated as shown in Eq. (21).

$$\text{RMSE} = \sqrt{\frac{\sum_{i=1}^{N} (\varepsilon_i - \hat{\varepsilon}_i)^2}{N}} \tag{21}$$

In Eq. (21), ε_i is an assumed complex permittivity value of ith cell, and $\hat{\varepsilon}_i$ is the reconstructed complex permittivity value of ith cell. N is the total number of cells used in model. Scattered field at receiver locations is obtained by solving forward problem. Now, noise is added to it, and complex permittivity value of each cell is reconstructed by solving inverse scattering problem.

6. INVERSE SCATTERING PROBLEM FORMULATION

Inverse scattering problem is solved with Levenberg-Marquardt method using [15, 20]. This method is also known as damped least square method. It is an iterative method in which matrix inversion is needed per iteration. Inverse scattering problem formulation without group theory is given using Eq. (22).

$$[\Delta\varepsilon] = \left(J_a^T J_a + \lambda \text{diag}\left(J_a^T J_a\right)\right)^{-1} J_a^T \left(\vec{E}^s - \hat{\vec{E}}^s\right) \tag{22}$$

In Eq. (22), J_a is Jacobian matrix. Matrix J_a is calculated by taking partial derivative of scattered electric field with respect to complex permittivity of each cell. $\vec{E}^s$ is scattered electric field column vector. $\vec{E}^s$ is obtained by solving forward problem of Eq. (6). $\hat{\vec{E}}^s$ is reconstructed scattered electric field. In the first iteration $\hat{\vec{E}}^s = B_1 R_g^{\varepsilon} \vec{E}$, where R_g^{ε} is an initial guess about matrix R^{ε}; $(\vec{E}^s - \hat{\vec{E}}^s)$ is known as residual; $[\Delta\varepsilon]$ represents change in complex permittivity at each of the iterations. λ is known as regularization parameter or damping factor. $[\Delta\varepsilon]$ is obtained by solving Equation (22) in each iteration. In order to get new value of R^{ε}, $[\Delta\varepsilon]$ is added to current value of R^{ε}. Inverse scattering problem formulation with group theory is given using Eq. (23).

$$[\Delta\varepsilon] = \left(J_a^T J_a + \lambda \text{diag}\left(J_a^T J_a\right)\right)^{-1} J_a^T \left(\vec{E}_b^s - \hat{\vec{E}}_b^s\right) \tag{23}$$

where, $\vec{E}_b^s$ is scattered electric field column vector. $\vec{E}_b^s$ is calculated after applying group theory. In Eq. (23), $\hat{\vec{E}}_b^s = B_{1b}(R_g^\varepsilon E)_b$ and $(R_g^\varepsilon E)_b = V(R_g^\varepsilon E)$. In Eq. (23), jacobian matrix is calculated using block diagonalized matrix $\vec{E}_b^s$. Computation time to solve Eq. (23) is reduced due to block diagonalized form of all matrices. Computation time to solve Eqs. (22) and (23) is given in [1] for single iteration. In this paper, overall computation time to solve inverse scattering problem is calculated with and without group theory. In order to compute overall simulation time, Eqs. (22) and (23) are solved with the same initial guess about matrix R. Number of iterations is 200 for both. Value of λ is calculated using general concepts given in [20].

7. RESULTS

Overhead time is also included in overall simulation time. The effect of group theory on overall simulation time versus number of cells is shown in Fig. 5. Overall simulation time is reduced due to symmetry exploitation using group theory.

The effect of group theory on RMSE in complex permittivity versus SNR is shown in Fig. 6. Fig. 6

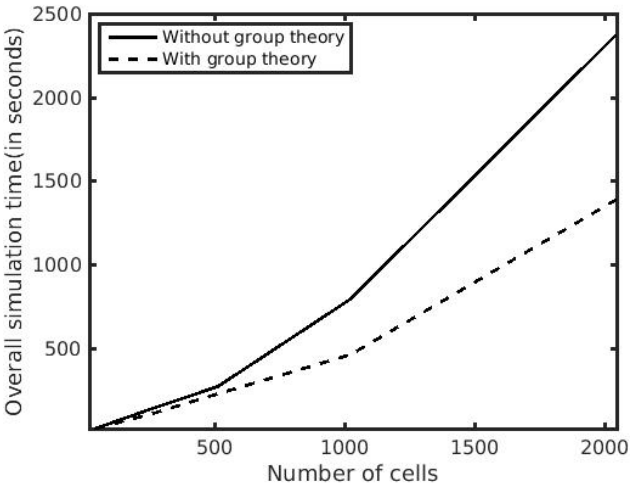

Figure 5. Overall simulation time vs. number of cells.

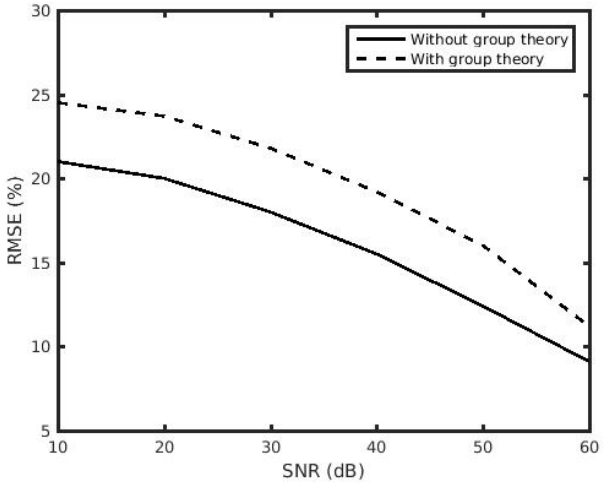

Figure 6. RMSE in complex permittivity vs. SNR (for 1024 cells).

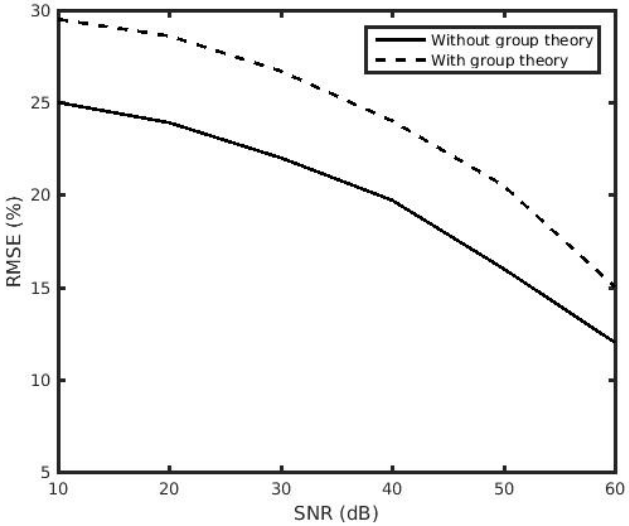

Figure 7. RMSE in complex permittivity vs. SNR (for 2048 cells).

shows the result for 1024-cell model. It clearly shows that RMSE without group theory is approximately same as RMSE with group theory for SNR greater than 50 dB. The effect of group theory on RMSE in complex permittivity versus SNR is shown in Fig. 7. Fig. 7 shows the result for 2048-cell model.

8. DISCUSSION AND CONCLUSION

Overall simulation time is reduced considerably when number of cells is more than 1000. Approximately 30% to 35% computation time is reduced by exploiting symmetry using group theory. In Levenberg-Marquardt algorithm, Equations (22) and (23) are solved in each of the iterations. Equation (22) is solved for the case without group theory, in which matrices are not in block diagonalized form. Matrix inversion of Equation (23) is faster than the matrix inversion of Equation (22) because group theory converts matrices in the block diagonalized form. Overall simulation time with group theory is less than that without group theory after 200 iterations. RMSE in complex permittivity is higher with group theory. This is considered as the price paid to get computational efficiency. However, for SNR greater than 50 dB, RMSE in complex permittivity without group theory is approximately same as RMSE in complex permittivity with group theory. Overall microwave image reconstruction time is reduced by exploiting symmetry using group theory.

REFERENCES

1. Patel, H. N. G. and D. Kumar, "Computationally efficient microwave imaging of human breast model using group theory," *Proc. IEEE MTTS IMaRC*, 81–84, 2015.
2. Rubæk, T. K., S. Oleksiy, and M. Peter, "Computational validation of a 3-D microwave imaging system for breast-cancer screening," *IEEE Transactions on Antennas and Propagation*, Vol. 57, No. 7, 2105–2115, July 2009.
3. Livesay, D. E. and K. M. Chen, "Electromagnetic fields induced inside arbitarily shaped biological bodies," *IEEE Transaction on Microwave Theory and Techniques*, Vol. 22, 1273–1280, 1974.
4. Hohmann, G. W. "Three dimensional induced polarization and electromagnetic modeling," *Geophysics*, Vol. 40, 305–324, 1975.
5. Ghodgaonkar, D. K., O. P. Gandhi, and M. J. Hagmann, "Estimation of complex permittivities of 3D inhomogeneous biological bodies," *IEEE Transactions on Microwave Theory and Techniques*, Vol. 31, 442–446, 1983.
6. Cohoon, D. K., "Reduction of the cost of solving an Integral Equation arising in electromagnetic scattering through the use of group theory," *IEEE Transactions on Antennas and Propagation*, Vol. 28, No. 1, 104–107, January 1980.
7. Ghodgaonkar, D. K. and R. Ismail, "Exploiting symmetry in electromagnetic imaging problems by using group representation theory," *Bull. Malaysian Math. Sc. Soc.*, Vol. 23, No. 1, 33–44, 2000.
8. Ney, M. M., A. M. Smith, and S. S. Stuchly, "A solution of electromagnetic imaging using pseudoinverse transformation," *IEEE Transactions on Medical Imaging*, Vol. 3, No. 4, 155–162, December 1984.
9. Pichot, C., L. Jofre, G. Peronnet, and J. Bolomey, "Active microwave imaging of Inhomogeneous bodies," *IEEE Transactions on Antennas and Propagation*, Vol. 33, No. 4, 416–425, April 1985.
10. Garnero, L., A. Franchois, J.-P. Hugonin, C. Pichot, and N. Joachimowicz, "Microwave Imaging-complex permittivity reconstruction by simulated annealing," *IEEE Transaction on Microwave Theory and Techniques*, Vol. 39, No. 11, 1801–1807, November 1991.
11. Belkebir, K., R. E. Kleinman, and C. Pichot, "Microwave imaging — location and shape reconstruction from multifrequency scattering data," *IEEE Transaction on Microwave Theory and Techniques*, Vol. 45, No. 4, 469–476, April 1997.
12. Caorsi, S., G. L. Gragnani, M. Pastorino, and M. Rebagliati, "A model driven approach to microwave diagnostics in biomedical applications," *IEEE Transactions on Microwave Theory and Techniques*, Vol. 44, No. 10, October 1996.

13. Pastorino, M., "Stochastic optimization methods applied to microwave imaging: A review," *IEEE Transactions on Antennas and Propagation*, Vol. 55, No. 3, 538–548, March 2007.
14. Fang, Q., P. M. Meaney, and K. D. Paulsen, "Singular value analysis of the jacobian matrix in microwave image reconstruction," *IEEE Transactions on Antennas and Wave Propagation*, Vol. 54, No. 8, August 2006.
15. Park, C.-S. and B.-S. Jeong, "Reconstruction of a high contrast and large object by using the hybrid algorithm combining a Levenberg-Marquardt algorithm and a genetic algorithm," *IEEE Transactions on Magnetics*, Vol. 35, No. 3, 1582–1585, May 1999.
16. Rubk, T., P. M. Meaney, P. Meincke, and K. D. Paulsen, "Nonlinear microwave imaging for breast-cancer screening using Gauss-Newton's method and the CGLS inversion algorithm," *IEEE Transactions on Antennas and Propagation*, Vol. 55, No. 8, 2320–2331, August 2007.
17. Andreuccetti, D., R. Fossi, and C. Petrucci, "An Internet resource for the calculation of the dielectric properties of body tissues in the frequency range 10 Hz–100 GHz," Website at http://niremf.ifac.cnr.it/tissprop/. IFAC-CNR, Florence, Italy, 1997. Based on data published by C. Gabriel, et al., in 1996.
18. Harrington, R. F., *Field Computation by Moment Methods*, IEEE Press, 1993.
19. Pozar, D. M., *Microwave Engineering*, John Wiley and Sons, 1989.
20. Dianat, S. A. and E. S. Saber, *Advanced Linear Algebra for Engineers with MATLAB*, CRC Press, 2009.